Journal of Thermal Analysis and Calorimetry, Vol. 78 (2004) 599–619

THE USE OF TG-FTIR TECHNIQUE FOR THE ASSESSMENT OF HYDROGEN BROMIDE EMISSIONS IN THE COMBUSTION OF BFRs

F. Barontini [1*], *K. Marsanich* [2] *and V. Cozzani* [3]

[1]Gruppo Nazionale per la Difesa dai Rischi Chimico-Industriali ed Ecologici, Consiglio Nazionale delle Ricerche, via Diotisalvi n. 2, 56126 Pisa, Italy
[2]Dipartimento di Ingegneria Chimica, Chimica Industriale e Scienza dei Materiali, Università degli Studi di Pisa, via Diotisalvi n. 2, 56126 Pisa, Italy
[3]Dipartimento di Ingegneria Chimica, Mineraria e delle Tecnologie Ambientali, Università degli Studi di Bologna, viale Risorgimento n. 2, 40136 Bologna, Italy

Abstract

The TG-FTIR technique was used in the present study to investigate the thermal degradation behaviour of materials containing brominated flame retardants under fire conditions. Time-temperature profiles and oxygen concentrations typical of selected fire scenarios were reproduced in the thermogravimetric analyzer, while the characterization of the gaseous products generated was performed by the simultaneous FTIR analysis. FTIR analysis combined with the use of specific calibration procedures allowed the quantitative estimation of the gaseous products evolved as a function of experimental conditions. The results obtained allowed the straightforward assessment and the comparison of the quantities of hydrogen bromide formed in the oxidation and thermal degradation of pure brominated flame retardants and of flame retarded materials of industrial interest. Hydrogen bromide yields resulted dependent on the experimental conditions used, such as oxygen concentration and heating rate. Although TG-FTIR experiments only provide a representation of the actual heterogeneous combustion products in real fire conditions, the coupled TG-FTIR technique proved to be a straightforward experimental methodology allowing one to obtain reference data on the nature and quantities of the macropollutants generated in a fire.

Keywords: brominated flame retardants, fire products, hyphenated techniques, quantitative evolved gas analysis, TG-FTIR

Introduction

Brominated compounds are widely used in industrial practice to improve the flame resistance of polymeric materials. Due to their high efficiency, compatibility and small influence on mechanical properties, brominated flame retardants (BFRs) have a broad application area. The production of brominated flame retardants increased from 145000 t/year

* Author for correspondence: E-mail: f.barontini@ing.unipi.it

1388–6150/2004/ $ 20.00

Akadémiai Kiadó, Budapest
Kluwer Academic Publishers, Dordrecht

in 1990 to 310000 t/year in 2000, mainly because of their use in the manufacture of epoxy resins used for printed circuit boards [1]. Thus, the growing use of BFRs is strongly linked to their widespread application in electronic appliances, such as personal computers, mobile phones and other high-tech large-diffusion products.

Despite the technical advantages of BFRs, their wide diffusion is causing an increasing concern on the possible formation of hazardous substances in case of thermal stress of these substances or of materials containing BFRs. In particular, fires involving brominated flame retarded materials are suspected be responsible of the formation and subsequent release in the environment of hazardous brominated compounds. The potential hazard coming from BFRs was considered so high that European Community decided strong limitations in their use and the ban of some of these compounds in 2002 [2]. However, an extensive investigation of the products formed in the thermal degradation and combustion of these compounds is still missing. Most of the former studies were dedicated to shed some light on the possible formation of extremely hazardous compounds, as polybrominated dibenzo-*p*-dioxins (PBDD) and polybrominated dibenzofurans (PBDF), in the oxidation of BFRs [3–15]. Only recently some studies were dedicated to the distribution of bromine among the thermal degradation products of the more common BFRs, as tetrabromobisphenol A (TBBA) and hexabromocyclododecane (HBCD) [16–24]. The results obtained evidenced that, apart the formation of extremely dangerous compounds as PBDD and PBDF, hazards may derive also from the formation of relevant quantities of hydrogen bromide and high molecular mass brominated compounds [25]. Thus, the investigation of products formed in fires involving BFRs or materials containing BFRs seems of utmost importance.

Predicting the hazardous substances and the relative yields that may be formed in fires results in a major problem, since fires involve a complex and interrelated array of physical and chemical phenomena. Many products may be generated due to incomplete decomposition and only partial oxidation of the substances involved. It is well known that temperature, residence time in the high temperature zone, and ventilation (oxygen availability) play significant roles in determining the final distribution of combustion products. Only full-scale experiments are able to reproduce the actual distribution of combustion products taking place in a fire [26]. Although small-scale tests provide only a simulation of real fire conditions, they are attractive due to the much lower times and costs required to carry out the experimental investigations. However, in laboratory-scale experiments, it is usually only possible to simulate separately the reactive chemical environments characteristic of various stages and types of real fire conditions in terms of temperature, presence or absence of flame, and oxygen supply. Nevertheless, a correct choice of experimental conditions may lead to obtain experimental yields at least representative of those evolved in the equivalent stages of full-scale fires. Thus, these data are often used as source terms to assess the consequences of the release in the environment of the hazardous substances generated. Several laboratory techniques were proposed to investigate the products of

fires. The more common experimental devices are horizontal fixed bed reactors, as the DIN furnace [27–30]. Thermogravimetry coupled to FTIR spectrometry for evolved gas analysis (TG-FTIR) was also proposed to obtain data on gaseous combustion products [30–42]. Lunghi *et al.* [43] recently proposed the use of temperature-time profiles derived from standard fire curves to simulate the combustion of solid materials in fires by TG techniques, and to obtain qualitative data on combustion products.

TG-FTIR techniques were used in the present study to simulate fire conditions and collect data on the dangerous substances formed in the combustion of brominated flame retardants. Time-temperature profiles and oxygen concentrations typical of selected fire scenarios were reproduced in the thermogravimetric analyzer, while the characterization of the gaseous products generated was performed by the simultaneous FTIR analysis. Both pure brominated flame retardants, specifically hexabromocyclododecane and tetrabromobisphenol A, and flame retarded materials of industrial interest, including laminated boards for printed circuits, were investigated. Hydrogen bromide was the main hazardous gaseous product generated for the systems considered in the study. The development and the use of a specific calibration procedure for the quantitative analysis of TG-FTIR data allowed an estimation of the quantities of hydrogen bromide evolved. Although TG-FTIR experiments only provide a representation of the actual heterogeneous combustion products in real fire conditions, the coupled TG-FTIR technique proved to be a straightforward experimental methodology allowing one to obtain at least reference data on the nature and quantities of the macropollutants generated in specific fire conditions.

Experimental

Materials

The following materials supplied by Aldrich (Milan, Italy) were used in the present study: 1,2,5,6,9,10-hexabromocyclododecane (HBCD), tetrabromobisphenol A (TBBA), brominated bisphenol A diglycidyl ether, brominated poly(4-vinylphenol), poly(styrene-*co*-4-bromostyrene-*co*-divinylbenzene), and poly(ethylene terephthalate) (PET) blended with a brominated aromatic compound as flame retardant.

Linear brominated epoxy resins were prepared by reaction of diglycidyl ether of bisphenol A (DGEBA, supplied by Shell) with tetrabromobisphenol A, using the procedures described elsewhere [44]. In the followings, the brominated epoxy resins will be identified by the DGEBA/TBBA molar ratio.

Flame retarded printed circuit board base materials were obtained from local manufacturers. Three printed circuit boards were selected and investigated in the present work. These were composed of an organic matrix on a glass fibre support. The analyses performed in the present study were carried out on powders obtained

Table 1 Bromine content of sample materials used in the present study

Sample	Bromine content/mass%
Hexabromocyclododecane	74.7
Tetrabromobisphenol A	58.8
Bisphenol A diglycidyl ether, brominated	47.1
Brominated epoxy resin DGEBA/TBBA 1.85	26.0
Brominated epoxy resin DGEBA/TBBA 2.75	20.4
Poly(4-vinylphenol) brominated	55.4
Poly(styrene-*co*-4-bromostyrene-*co*-divinylbenzene)	20.5
PET blended with brominated compound	8.5
Electronic board A	6.9
Electronic board B	6.7
Electronic board C	6.0

milling the samples in liquid nitrogen. These will be denoted as electronic boards A, B and C in the followings.

Table 1 summarizes the materials used in the present study and reports their bromine content, determined by elemental analysis.

Techniques

Simultaneous thermogravimetric (TG) and differential scanning calorimetry (DSC) data were obtained using a Netzsch STA 409/C thermoanalyzer. Sample masses between 5 and 50 mg were employed in experimental runs. FTIR measurements were carried out using a Bruker Equinox 55 spectrometer. TG-FTIR simultaneous measurements for the on-line analysis of volatile compounds formed during TG runs were carried out coupling the FTIR spectrometer to the Netzsch TG using a 2 mm internal diameter teflon tube. The 800 mm long transfer line and the head of the TG balance were heated at a constant temperature of 200°C to limit the condensation of volatile decomposition products. FTIR measurements were carried out with a MCT detector in a specifically developed low volume gas cell (8.7 mL) with a 123 mm pathlength, heated at a constant temperature of 250°C. The gas flow from the TG outlet to the IR gas cell was of 60 mL min^{-1} (at 25°C and 101.3 kPa) and a mean value of 30 s could be estimated for the residence time of evolved gases in the transfer line. This value was assumed as the time delay correction to be used for the comparison of TG and IR results. During TG-FTIR runs, spectra were collected at 4 cm^{-1} resolution, co-adding 16 scans per spectrum. This resulted in a time resolution of 9.5 s.

Simulation of combustion conditions in the TG analyzer

Several investigations evidenced that under standard conditions there is a specific relationship between time and temperature of solid materials involved in a fire taking place in a confined environment. This led to the development of several standard time-temperature curves for fire tests on building materials [45]. A widely used reference time-temperature curve is reported by ASTM E119 standard, that gives a set of temperature values as a function of time from the beginning of the fire [46]. The ASTM E119 curve is used to represent a severe building fire, and may thus be used as well for the simulation of a warehouse fire involving the storage of chemicals.

Thus, the ASTM E199 reference curve was used in the present study as a representative time-temperature profile to investigate the gaseous products evolved in fire conditions by TG-FTIR tests. The time-temperature profile defined in the Standard Test Methods E119 was reproduced in the Netzsch STA 409/C thermal analyzer. Figure 1 shows a comparison between the standard ASTM E119 curve and the temperatures measured in the TG furnace during a standard experimental run. A sufficient correspondence is evidenced in the figure between the furnace time-temperature profile and that of the standard curve. The experimental runs reported in the present study were performed using the experimental time-temperature profile reported in Fig. 1.

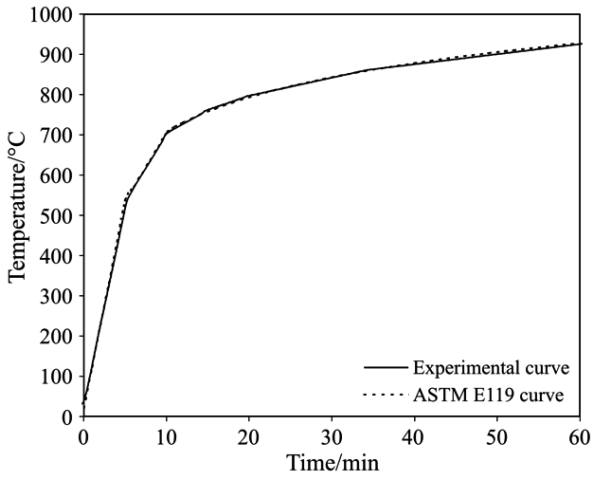

Fig. 1 Simulation of combustion conditions in the TG analyzer: comparison between the experimental temperature recorded in the TG furnace and the standard ASTM E119 curve

A purge gas flow was used during experimental runs in order to control the reaction environment. Specific oxygen/nitrogen mixtures were employed to reproduce the combustion conditions characteristic of selected types or stages of fire, following the approach suggested by the International Organization for Standardization (as re-

ported in Technical Report ISO/TR 9122-4) [28]. A 15% oxygen concentration was used to reproduce non-flaming oxidative conditions, while a 100% nitrogen flow was employed to simulate non-flaming pyrolytic conditions.

Results and discussion

Quantitative determination of hydrogen bromide evolved in TG-FTIR runs

The results of TG-FTIR runs were analyzed in order to estimate the quantities of selected gaseous products formed in the TG analyzer during the thermal degradation of the brominated materials under investigation. The analysis was specifically addressed to the determination of the quantities of hydrogen bromide formed in oxidizing conditions.

The starting point of the procedure used for FTIR quantitative data analysis was based on an integral form of the Lambert-Beer law, relating the concentration of the compound of interest to the integral of absorbance over a selected wavenumber interval:

$$I=\int_{\tilde{\nu}_1}^{\tilde{\nu}_2} A(\tilde{\nu})\mathrm{d}\tilde{\nu}=c\int_{\tilde{\nu}_1}^{\tilde{\nu}_2}\varepsilon(\tilde{\nu})\,l\,\mathrm{d}\tilde{\nu}=Kc \qquad (1)$$

where A is the measured absorbance, I the integral value, ε the extinction coefficient of the gaseous compound, l the optical pathlength used in the measurement, c the concentration and $(\tilde{\nu}_1, \tilde{\nu}_2)$ the wavenumber interval selected for the measurement. The value of K depends on the compound considered, the wavenumber interval, the temperature of the gas, the optical pathlength and the instrument resolution. Moreover, K is also dependent on concentration, unless deviations from the Lambert–Beer law may be neglected [47, 48]. Thus a reliable value of K may be obtained only by a calibration procedure.

Equation (1) may be used to qualitatively monitor the evolution of selected gaseous compounds as function of time or of the temperature of the TG furnace, if wavenumber absorption intervals of the compounds of interest reasonably free of additional contributions from the other species are present. The approach may still be used even if it is not possible to identify independent absorption intervals for the species of interest, provided that a deconvolution method is used for the estimation of absorption due to the compound of interest in Eq. (1) [49, 50].

Quantitative data may be obtained from the above approach by the use of calibration procedures. The conventional technique used for quantitative FTIR determinations of gaseous compounds is based on a calibration performed using different gaseous mixtures containing known concentrations of the compound of interest [48, 51–53]. Concentration-based calibration procedures may be directly based on Eq. (1). Selecting single or multiple wavenumber intervals characteristic of the compound of interest, K may be estimated as a function of concentration. However, the use of concentration-based FTIR calibration techniques is time-consuming and costly. If calibration standards are used as re-

ceived, a high number of different concentration standards is required. If calibration standards are diluted in the system to achieve different concentrations, errors may be introduced. Furthermore safety and disposal problems may arise if the compounds of interest are toxic or corrosive substances, as in the case of hydrogen bromide. To limit these problems, pulse calibration methods were developed for TG-FTIR devices [54]. These are based on sending a gas pulse containing a known quantity of the compound of interest to the FTIR analyzer. The total moles n of the compound of interest in the gas pulse may be related to the concentration in the FTIR gas cell by the following expression:

$$n=\int_{t_1}^{t_2} F c \mathrm{d}t \tag{2}$$

where F is the total volumetric gas flow rate of the TG carrier gas at the actual gas temperature in the measurement cell, and (t_1,t_2) is a time interval wider than the duration of the gas pulse. Integrating Eq. (1) over time interval (t_1,t_2) yields the following expression:

$$D=\int_{t_1}^{t_2}\left[\int_{\tilde{\nu}_1}^{\tilde{\nu}_2} A(\tilde{\nu})\mathrm{d}\tilde{\nu}\right]\mathrm{d}t=\int_{t_1}^{t_2} Kc\mathrm{d}t \tag{3}$$

The value of integral D may be related to n as follows:

$$D=\frac{\int_{t_1}^{t_2} Kc\mathrm{d}t}{\int_{t_1}^{t_2} Fc\mathrm{d}t}n=K'n \tag{4}$$

where K' is a correlation factor that depends on n and on the operating conditions of the experimental run. The value of D may be measured, thus allowing the estimation of K' as a function of n. However, if deviations from the Lambert–Beer law are negligible, and if the same constant carrier gas flowrate is used during calibrations and experiments, K' is a constant that may be easily related to K:

$$D=K'n=\frac{K}{F}n \tag{5}$$

Two different pulse-calibration techniques are available for TG-FTIR analyzers: gas-pulse and vaporization methods. The gas-pulse calibration method is based on the use of a gas injection device consisting in a rotary sampling valve allowing the TG carrier gas to purge a known-volume loop, previously filled with a calibration gas of known composition. The vaporization method consists in the vaporization of liquid solutions of the compound of interest in the TG analyzer of the TG-FTIR device. The use of solutions of different concentration and of samples having different

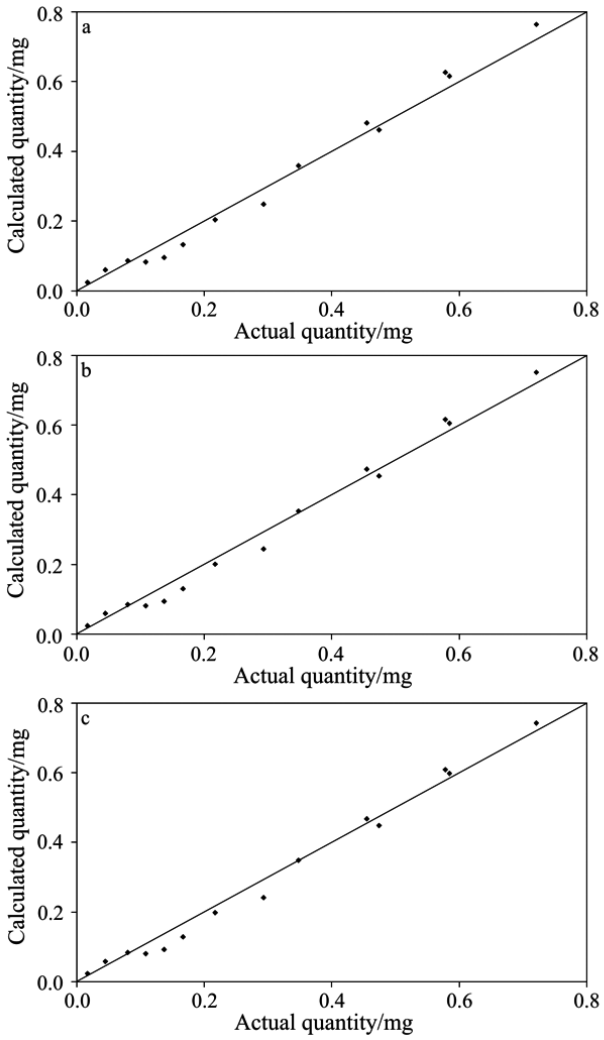

Fig. 2 Comparison of actual and calculated quantities of ammonia from a – concentration-based calibration, b – gas-pulse calibration and c – vaporization-based calibration

masses allows the vaporization of different quantities of the compound of interest, that are carried to the IR measurement cell by the TG carrier gas flow. The reliability of these simplified calibration techniques was assessed and compared to the results of the conventional concentration method. Figure 2 shows an example of the results obtained for ammonia. Negligible differences resulted in the absolute quantities estimated by the three techniques, and no relevant differences were found in the order of magnitude of experimental errors in the range of concentrations and of quantities ex-

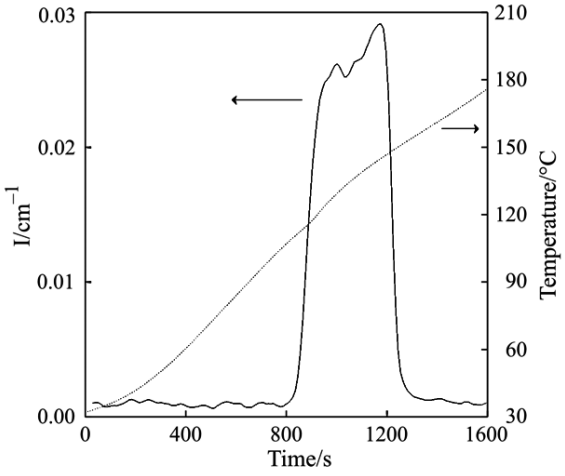

Fig. 3 Integrated absorbance profile of hydrogen bromide during a calibration run performed vaporizing a 6.5 mol% hydrobromic acid solution

plored. The mean relative error always resulted less than 5%. Thus, pulse calibration techniques may be fruitfully used to obtain quantitative data on evolved gaseous products in TG-FTIR applications.

The vaporization-based method was used in the present study for hydrogen bromide calibration. Hydrogen bromide solutions in water were employed in calibration runs. About 15–25 mg of hydrobromic acid solutions were vaporized in the TG apparatus, performing constant heating rate (5°C min^{-1}) runs from 25 to 200°C, using a 60 mL min^{-1} pure nitrogen flow. The 2498–2516 cm^{-1} wavenumber interval was selected for HBr determination. Figure 3 shows the typical results obtained in calibration

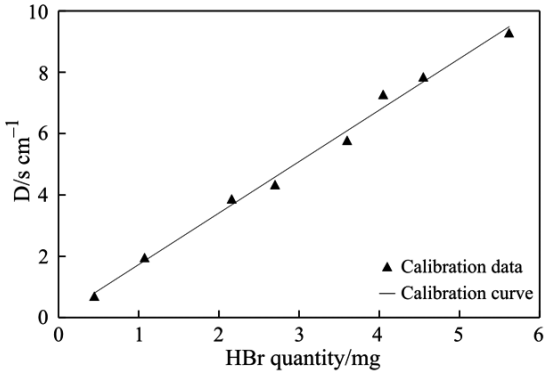

Fig. 4 Calibration data used for the quantitative determination of HBr formed in TG-FTIR runs

runs. The sample temperature and the value of the integrated absorbance, *I*, calculated for hydrogen bromide are reported with respect to time for a run performed vaporizing 18.95 mg of a 6.5 mol% hydrobromic acid solution. As evident from the results of Fig. 3, the vaporization of the sample generates a pulse of the compound of interest. For each calibration run performed, the values of *I* were calculated on the wavenumber interval selected for HBr, and were integrated with respect to time, thus obtaining the value of *D* in Eq. (3). The values obtained for integral *D* from the analysis of calibration runs were plotted as a function of the quantity of HBr present in the sample vaporized. As shown by the results reported in Fig. 4, a linear dependence of the value of *D* with respect to HBr amount was found. Thus a linear calibration curve was obtained, relating the value of *D* to hydrogen bromide quantity. The linearity of the calibration curve suggests that, as expected, limited deviations from the Lambert–Beer law are present in the concentration range explored in experimental runs. The best-fit linear relation obtained between the value of *D* and HBr quantity was used to estimate the amount of HBr formed during TG-FTIR thermal degradation runs.

Thermal degradation behaviour of materials containing brominate flame retardants

Experimental TG-FTIR runs were performed on the brominated materials listed in the experimental section. The time-temperature profile reported in Fig. 1 was used to simulate fire conditions. Experimental runs were carried out under both oxidative (15 mol% O_2 in N_2) and pyrolytic (100% N_2) conditions. Figure 5 shows the typical results obtained in TG-FTIR runs. Unless otherwise stated, the data reported in this and in the following figures were calculated as the mean of at least three experimental runs. Relative differences in mass loss with respect to time in different runs were always lower than 2%. The figure reports the sample mass loss, the differential thermogravimetric curve (DTG) and the qualitative emission profile of hydrogen bromide, obtained from FTIR data. The FTIR simultaneous measurements allowed the characterization of volatile products generated during TG runs. Figure 6 shows the results of FTIR on-line analysis of the volatiles evolved in the TG run in oxygen 15% reported in Fig. 5. The IR spectra recorded by the system are reported as a function of time. Using FTIR data such as those reported in Fig. 6 and the procedures described above qualitative emission profiles as a function of time were obtained for the gaseous compounds evolved. In particular, hydrogen bromide emission could be monitored during the experimental runs performed. Figure 5c shows the recorded emission profiles of hydrogen bromide during the experimental runs performed.

Data as those shown in Figs 5 and 6 were collected for all the materials considered in the present study. The results reported in Fig. 5 were obtained for the 1.85 DGEBA/TBBA linear brominated epoxy resin, an intermediate used in the manufacture of printed circuit boards. The mass loss data reported in Fig. 5a evidence the presence of a main degradation step between 350 and 500°C, both in inert and oxidizing conditions. In the presence of oxygen, a second mass loss step occurred at higher

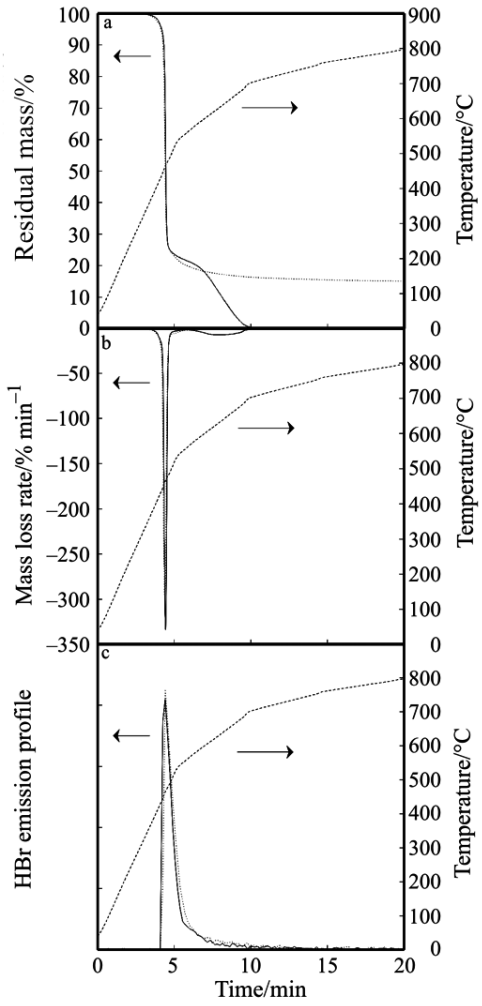

Fig. 5 Results of TG-FTIR runs performed on the DGEBA/TBBA 1.85 resin (ASTM E119 conditions; continous lines: oxygen 15%; dotted lines: nitrogen 100%). a – mass loss data, b – mass loss rate data, c – hydrogen bromide emission profile

temperatures (600–700°C). The FTIR results in oxidizing conditions, shown in Fig. 6, confirmed the presence of a first degradation step, during which a complex mixture of products including hydrogen bromide (2780–2400 cm^{-1}), carbon dioxide (2400–2240 cm^{-1}), carbon monoxide (2235–2030 cm^{-1}) and methane (3026–3001 cm^{-1}), is generated. The emission of carbon dioxide and carbon monoxide was also detected during the second mass loss step evidenced in Fig. 5 for the run performed in the presence of oxygen. Figure 5c shows the recorded emission profiles of hydrogen bromide. Hydrogen bromide concentration in the gas outflow from the TG analyzer shows a single

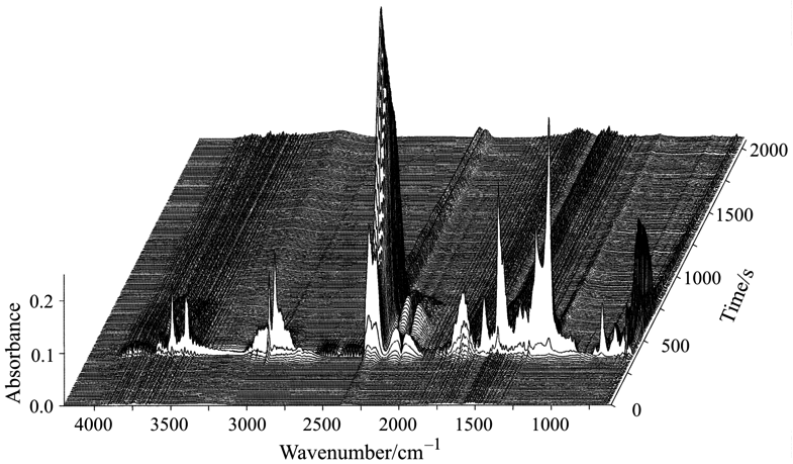

Fig. 6 FTIR spectra collected during the on-line analysis of the volatiles evolved in the combustion of the DGEBA/TBBA 1.85 resin (ASTM E119 conditions, oxygen 15%)

peak under both oxidative and pyrolytic conditions, in correspondence of the maximum of the sample mass loss rate during the first mass loss step. Thus it may be concluded that the first thermal degradation step of this material in the experimental conditions of the present study is not influenced by the presence of oxygen. On the other hand, in the presence of oxygen a second mass loss peak appears at higher temperatures, probably due to the oxidation of the solid residue formed in the first decomposition stage. As a matter of fact, the pyrolytic degradation of the brominated epoxy resin yielded a black solid residue, while no residue was present in the crucible at the end of experimental runs performed in oxidizing environment.

A qualitatively similar behaviour was shown by the other brominated materials considered in the present study. Detailed data about decomposition temperatures and volatile loss could be obtained from the analysis of the experimental runs performed. Tables 2 and 3 report the maximum mass loss rate temperature and the residual mass at the end of the main degradation step experienced in the experimental conditions explored in the present work. As evident from the results shown in Table 2, the presence of oxygen does not affect significantly the decomposition temperature range of the samples analyzed (with the exception of poly(styrene-*co*-4-bromostyrene-*co*-divinylbenzene)). The mass of the residue formed in the main degradation step was not influenced by the reaction environment for some of the materials considered, while for others increased in oxidative conditions. In 15% oxygen all the samples evidenced a further mass loss step at higher temperatures, with emission of carbon monoxide and carbon dioxide. This may well correspond to the oxidation of the solid residue formed in the first decomposition stage. On the other hand, only a slight mass loss was experienced at the correspondent temperatures in nitrogen atmosphere.

Table 2 Maximum mass loss rate temperature recorded for the materials investigated in the present study

Sample	Maximum mass loss rate temperature/°C			
	ASTM E119 standard conditions		Constant heating rate/10°C min^{-1}	
	O_2 15%	N_2 100%	O_2 15%	N_2 100%
Hexabromocyclododecane	323	324	261	266
Tetrabromobisphenol A	416	408	337	337
Bisphenol A diglycidyl ether, brominated	446	453	373	376
Brominated epoxy resin DGEBA/TBBA 1.85	468	459	375	375
Brominated epoxy resin DGEBA/TBBA 2.75	465	465	381	387
Poly(4-vinylphenol) brominated	404	402	328	329
Poly(styrene-*co*-4-bromostyrene-*co*-divinylbenzene)	530	540	397	441
PET blended with brominated compound	515	514	418	424
Electronic board A	392	392	315	315
Electronic board B	377	385	314	315
Electronic board C	377	387	314	315

Table 3 Residual mass at the end of the first degradation step for the materials investigated in the present study

Sample	Residual mass/mass%			
	ASTM E119 standard conditions		Constant heating rate/10°C min^{-1}	
	O_2 15%	N_2 100%	O_2 15%	N_2 100%
Hexabromocyclododecane	6	6	9	8
Tetrabromobisphenol A	28	27	35	31
Bisphenol A diglycidyl ether, brominated	24	20	30	28
Brominated epoxy resin DGEBA/TBBA 1.85	25	25	29	29
Brominated epoxy resin DGEBA/TBBA 2.75	22	21	28	24
Poly(4-vinylphenol) brominated	43	42	51	46
Poly(styrene-*co*-4-bromostyrene-*co*-divinylbenzene)	7	6	21	8
PET blended with brominated compound	39	40	46	43
Electronic board A	68	67	72	70
Electronic board B	73	69	82	73
Electronic board C	73	71	81	75

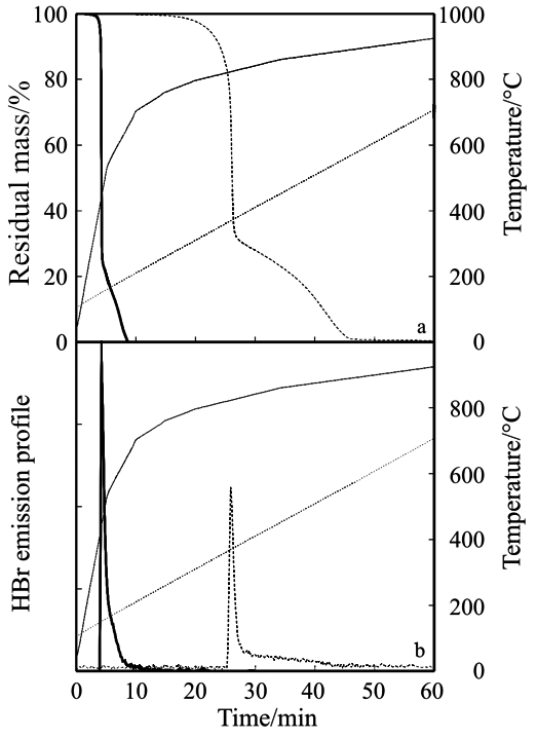

Fig. 7 Results of TG-FTIR runs performed on brominated bisphenol A diglycidyl ether (oxygen 15%; continuous lines: ASTM E119 conditions; dashed lines: 10°C min^{-1} constant heating rate run). a – mass loss data, b – hydrogen bromide emission profile

Hydrogen bromide was identified among the complex mixture of volatile products evolving during the degradation process in all the experimental runs performed. Hydrogen bromide emission profiles similar to those reported in Fig. 5c were recorded for all the materials investigated.

Influence of the heating rate

In order to investigate the influence of the temperature-time profile on the thermal degradation behaviour, 10°C min^{-1} constant heating rate runs were performed and the results were compared to those obtained using the temperature-time profile reported in Fig. 1. Figure 7 reports the results of the comparison for brominated bisphenol A diglycidyl ether. Sample mass loss and hydrogen bromide emission profiles in TG-FTIR runs performed in 15% oxygen are shown in the figure as a function of time. The temperature-time profile clearly affects both the mass loss behaviour and the hydrogen bromide emission. This is more clearly evidenced in Fig. 8, which reports the TG and DTG curves as a function of the sample temperature. The differ-

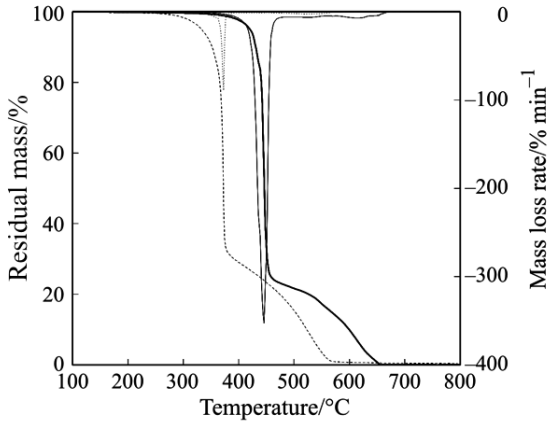

Fig. 8 Results of TG runs performed on brominated bisphenol A diglycidyl ether (oxygen 15%; continuous lines: ASTM E119 conditions; dashed lines: 10°C min^{-1} constant heating rate run)

ent temperature-time profiles result in different thermal degradation temperature ranges, different volatile losses, and different mass loss rates. Similar results were obtained for all the materials investigated in the present study, and are summarized in Tables 2 and 3. As expected, increasing heating rates result in increasing decomposition temperatures. A careful inspection of the data reported in Table 3 reveals that the mass of the residue formed in the first thermal degradation step increases with decreasing heating rates. Differences up to 14 mass% were obtained for the mass loss in the first thermal degradation step. Thus, these results suggest that the use of the ASTM standard fire curve is an important factor to obtain results more representative of the products formed in actual fire conditions.

Quantities of hydrogen bromide evolved in the degradation of brominated flame retarded materials

The use of the above discussed calibration procedure and of the calibration data shown in Fig. 4 allowed a quantitative estimation of hydrogen bromide evolved in the degradation of the brominated materials investigated. The results of TG-FTIR runs performed using the temperature-time profile shown in Fig. 1 were analyzed, and the results of the quantitative determinations performed are shown in Table 4. The quantities of hydrogen bromide generated in TG-FTIR runs are reported in the Table for all the materials investigated in the present study. The values in Table 4 were obtained as the mean of at least three experimental runs, with relative errors being less than 5%. The relative amounts of bromine initially present in the sample and converted to HBr were included in Table 4. These were calculated on the basis of the initial bromine content of the sample, shown in Table 1.

Table 4 Quantities of HBr formed in TG-FTIR runs (ASTM E119 standard conditions)

Sample	g HBr formed/100 g sample		Bromine released as HBr/%	
	O_2 15%	N_2 100%	O_2 15%	N_2 100%
Hexabromocyclododecane	56.0	59.1	74.0	78.1
Tetrabromobisphenol A	34.6	33.8	58.2	56.9
Bisphenol A diglycidyl ether, brominated	26.6	24.6	55.9	51.6
Brominated epoxy resin DGEBA/TBBA 1.85	15.0	14.1	57.1	53.6
Brominated epoxy resin DGEBA/TBBA 2.75	10.1	9.5	48.7	46.0
Poly(4-vinylphenol) brominated	42.0	42.0	74.8	74.8
Poly(styrene-*co*-4-bromostyrene-*co*-divinylbenzene)	4.1	2.0	19.6	9.5
PET blended with brominated compound	1.6	0.7	18.1	8.2
Electronic board A	4.6	4.2	66.8	60.1
Electronic board B	5.3	5.4	77.5	79.2
Electronic board C	4.5	3.8	74.4	63.3

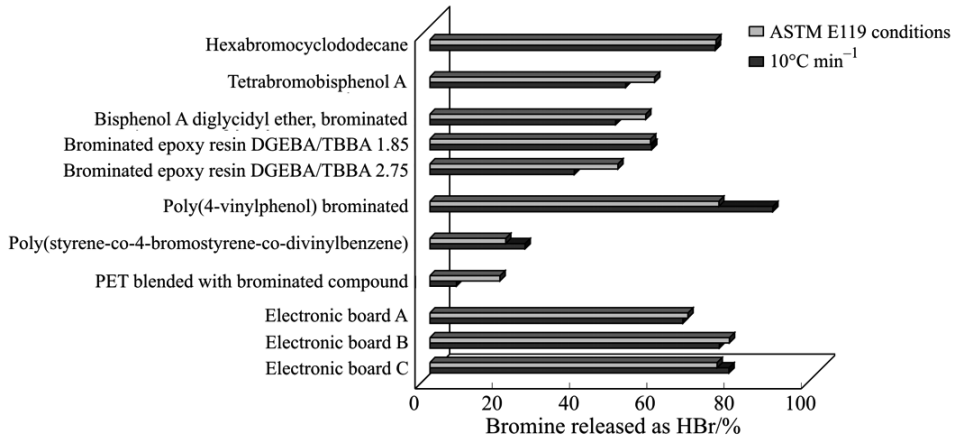

Fig. 9 Quantities of HBr formed in TG-FTIR runs (oxygen 15%) performed using different temperature-time profiles

The results reported in Table 4 clearly point out that the involvement in fires of brominated materials may cause severe consequences due to the emission of large quantities of hydrogen bromide. More than 50% of bromine present in the sample is released as hydrogen bromide for most of the materials analyzed, and HBr quantities as high as 59 g per 100 g of sample may be formed.

The quantitative assessment of hydrogen bromide emissions was performed under both oxidative and pyrolytic conditions. As shown in Table 4, the presence of oxygen affects the quantities of hydrogen bromide formed. However, a general trend was not identified for all the samples. The quantities of bromine converted to HBr were found as well to increase or decrease in the presence of oxygen, depending on the sample material. Two contrasting factors may be responsible of this behaviour: on one hand, the presence of oxidizing conditions may lead to the conversion of bromine present in the sample to molecular Br_2. However, the presence of oxygen also causes a more severe demolition of the sample structure, potentially leading to the formation of higher quantities of volatile products, as hydrogen bromide.

The influence of the time-temperature profile on the quantities of hydrogen bromide generated is shown in Fig. 9. Also in this case, increases as well as decreases were found for the HBr yields among the different samples. The results reported in Table 4 and Fig. 9 evidence that experimental conditions, such as time-temperature profile and oxygen concentration may affect the yields of the hazardous gaseous products formed. Furthermore, the effect of the heating rate and of the oxygen concentration on HBr yields strongly depends on the characteristics of the sample material considered. Hence, the results obtained point out that an efficient simulation of fire conditions, such as the sample heating rate and the oxygen availability, is neces-

sary to obtain representative data for the quantitative distribution of hazardous gaseous emissions in fires.

Conclusions

The use of specifically developed calibration procedures allowed the qualitative and quantitative estimation by TG-FTIR technique of the gaseous products evolved in the thermal degradation of materials containing brominated flame retardants. Hydrogen bromide was found to be present in relevant quantities among the evolved gaseous products. Hydrogen bromide yields resulted highly dependent on the characteristics of the brominated substrate and on the experimental conditions used in experimental runs, such as oxygen concentration and heating rate. However, for some of the materials considered in the present study, hydrogen bromide yields were as high as 60% by mass of the sample. These data pointed out that the involvement in fires of brominated materials may cause the formation and release of toxic fumes containing large amounts of hydrogen bromide, that may result in a major hazard.

The efficient simulation of the selected fire conditions thus appears a critical factor if a quantitative assessment of hazardous product emission is required. Although TG-FTIR experiments only provide a representation of the actual heterogeneous combustion products in real fire conditions, the TG-FTIR technique proved to be a straightforward experimental methodology to achieve reference data on the nature and quantities of the macropollutants generated in specific fire conditions.

* * *

The authors gratefully acknowledge financial support from CNR – Gruppo Nazionale di Ricerca per la Difesa dai Rischi Chimico-Industriali ed Ecologici.

References

1 Directive 2002/95/EC of the European Parliament and of the Council of 27 January 2003 on the restriction of the use of certain hazardous substances in electrical and electronic equipment, Official Journal of the European Union, L 37/19, 13. 2. 2003.
2 Directive 2002/96/EC of the European Parliament and of the Council of 27 January 2003 on waste electrical and electronic equipment (WEEE), Official Journal of the European Union, L 37/24, 13. 2. 2003.
3 H. Thoma, S. Rist, G. Hauschulz and O. Hutzinger, Chemosphere, 15 (1986) 649.
4 H. R. Buser, Environ. Sci. Technol., 20 (1986) 404.
5 D. Bienek, M. Bahadir and F. Korte, Heterocycles, 28 (1989) 719.
6 R. Dumler, H. Thoma, D. Lenoir and O. Hutzinger, Chemosphere, 19 (1989) 2023.
7 J. Thies, M. Neupert and W. Pump, Chemosphere, 20 (1990) 1921.
8 R. Luijk, H. Wever, K. Olie, H. A. J. Govers and J. J. Boon, Chemosphere, 23 (1991) 1173.
9 R. C. Striebich, W. A. Rubey, D. A. Tirey and B. Dellinger, Chemosphere, 23 (1991) 1197.
10 R. Luijk and H. A. J. Govers, Chemosphere, 25 (1992) 361.

11 R. Dumler-Gradl, D. Tartler, H. Thoma and O. Vierle, Organohalogen Compd., 24 (1995) 101.
12 M. Riess, T. Ernst, R. Popp, B. Müller, H. Thoma, O. Vierle, M. Wolf and R. van Eldik, Chemosphere, 40 (2000) 937.
13 S. Sakai, J. Watanabe, Y. Honda, H. Takatsuki, I. Aoki, M. Futamatsu and K. Shiozaki, Chemosphere, 42 (2001) 519.
14 G. Söderström and S. Marklund, Environ. Sci. Technol., 36 (2002) 1959.
15 H. Wichmann, F. T. Dettmer and M. Bahadir, Chemosphere, 47 (2002) 349.
16 A. Factor, J. Polym. Sci., Polym. Chem. Ed., 11 (1973) 1691.
17 E. R. Larsen and E. L. Ecker, J. Fire Sci., 4 (1986) 261.
18 F. Barontini, V. Cozzani and L. Petarca, Ind. Eng. Chem. Res., 40 (2001) 3270.
19 F. Barontini, V. Cozzani, A. Cuzzola and L. Petarca, Rapid Commun. Mass Spectrom., 15 (2001) 690.
20 F. Barontini, V. Cozzani and L. Petarca, J. Anal. Appl. Pyrol., 70 (2003) 353.
21 E. J. C. Borojovich and Z. Aizenshtat, J. Anal. Appl. Pyrol., 63 (2002) 105.
22 A. Hornung, A. I. Balabanovich, S. Donner and H. Seifert, J. Anal. Appl. Pyrol., 70 (2003) 723.
23 F. Barontini, K. Marsanic, L. Petarca and V. Cozzani, Ind. Eng. Chem. Res., 43 (2004) 1952.
24 F. Barontini, V. Cozzani, K. Marsanich, V. Raffa and L. Petarca, J. Anal. Appl. Pyrol., 72 (2004) 41.
25 F. Barontini, V. Cozzani, L. Petarca and S. Zanelli, Proc. 10th Int. Symp. on Loss Prevention and Safety Promotion in the Process Industries, Elsevier, Amsterdam 2001, p. 1251.
26 M. Molag, H. Bartelds and D. De Weger, Toxic products from pesticide fires, Report 92-366/112327-17897, TNO, Apeldoorn (NL) 1992.
27 F. H. Prager, J. Fire Sci., 6 (1988) 3.
28 Technical Report ISO/TR 9122-4, Toxicity testing of fire effluents – Part 4: The fire model (furnaces and combustion apparatus used in small-scale testing), International Organization for Standardization, Switzerland 1993.
29 L. Pecori, Bs. Thesis in Chemical Engineering, University of Pisa, Pisa, Italy 2000.
30 J. Bak, FTIR-PTGA Gas Analysis of Solid Fuels, Risø-R-825(EN), Risø National Laboratory, Roskilde, Denmark 1995.
31 P. S. Bhandare, B. K. Lee and K. Krishnan, J. Thermal Anal., 49 (1997) 361.
32 M. Krunks, T. Leskelä, R. Mannonen and L. Niinistö, J. Therm. Anal. Cal., 53 (1998) 355.
33 N. G. Fisher and J. G. Dunn, J. Therm. Anal. Cal., 56 (1999) 43.
34 I. Pitkanen, J. Huttenen, H. Halttunen and R. Vesterinen, J. Therm. Anal. Cal., 56 (1999) 1253.
35 A. Zanier, J. Therm. Anal. Cal., 56 (1999) 1389.
36 M. Herrera, G. Matuschek and A. Kettrup, J. Therm. Anal. Cal., 59 (2000) 385.
37 R. Mrozek, Z. Rzaczynska and M. Sikorska-Iwan, J. Therm. Anal. Cal., 63 (2001) 839.
38 G. Janowska and L. Ślusarski, J. Therm. Anal. Cal., 65 (2001) 205.
39 J. Suuronen, I. Pitkänen, H. Halttunen and R. Moilanen, J. Therm. Anal. Cal., 69 (2002) 359.
40 R. Kunze, B. Schartel, M. Bartholmai, D. Neubert and R. Schriever, J. Therm. Anal. Cal., 70 (2002) 897.
41 T. Kaljuvee, R. Kuusik and A. Trikkel, J. Therm. Anal. Cal., 72 (2003) 393.
42 S. Materazzi and R. Curini, Appl. Spectroscop. Rev., 36 (2001) 1.
43 A. Lunghi, D. Faedo, L. Gigante, C. Di Bari, A. Pugliano and P. Cardillo, Riv. Comb., 55 (2001) 213.
44 F. Barontini, V. Cozzani and L. Petarca, Ind. Eng. Chem. Res., 39 (2000) 855.

45 F. P. Lees, Loss Prevention in the Process Industries, 2nd Ed., Butterworth–Heineman, London 1986, p. 16/293.
46 ASTM E 119, Standard Test Methods for Fire Tests of Building Construction and Materials, 1995 Annual Book of ASTM Standards, Vol. 04.07, ASTM, Philadelphia 1995, p. 436.
47 W. J. Potts Jr., Chemical Infrared Spectroscopy, John Wiley & Sons, New York 1963.
48 J. Bak and A. Larsen, Appl. Spectrosc., 49 (1995) 437.
49 J. R. Ferraro and K. Krishnan, Fourier Transform Infrared Spectroscopy, Academic Press, New York 1985.
50 D. M. Haaland, Practical Fourier Transform Infrared Spectroscopy, Academic Press, San Diego 1990.
51 D. E. Pivonka, Appl. Spectrosc., 45 (1991) 597.
52 A. Hakuli, A. Kytokivi, E. L. Lakomaa and O. Krause, Anal. Chem., 67 (1995) 1881.
53 V. Seebauer, J. Petek and G. Staudinger, Fuel, 76 (1997) 1277.
54 K. Marsanich, F. Barontini, V. Cozzani and L. Petarca, Thermochim. Acta, 390 (2002) 153.